

Proximity Operator of the ℓ_1 over ℓ_2 Function

Lixin Shen¹ and Guohui Song^{2*}

¹Department of Mathematics, Syracuse University, Syracuse, NY 13244, USA.

²Department of Mathematics and Statistics, Old Dominion University, Norfolk, VA 23529, USA.

*Corresponding author(s). E-mail(s): gsong@odu.edu;
Contributing authors: lshen03@syr.edu;

Abstract

We study the proximity operator of the nonconvex, scale-invariant ratio $h(\mathbf{x}) = \|\mathbf{x}\|_1/\|\mathbf{x}\|_2$ and show it can be computed exactly in any dimension. By expressing $\mathbf{x} = \mathbf{r}\mathbf{u}$ and exploiting sign and permutation invariance, we reduce the proximal step to a smooth optimization of a rank-one quadratic over the non-negative orthant of the unit sphere. We prove that every proximal point arises from a finite candidate set indexed by $\mathbf{k} \in \{1, \dots, n\}$: the active subvector is a local, but nonglobal, minimizer on \mathbb{S}^{k-1} characterized by the roots of an explicit quartic. This yields closed-form candidates, an exact selection rule, and a necessary and sufficient existence test. Building on these characterizations, we develop practical algorithms, including an $\mathcal{O}(n)$ implementation via prefix sums and a pruning criterion that avoids unnecessary quartic solves. The method returns all proximal points when the prox is non-unique, and in experiments it attains strictly lower objective values than approaches that guess sparsity or rely on sphere projections with limited scalability.

Keywords: Proximity operator, l1 over l2, manifold optimization, nonconvex optimization, sparse modeling

1 Introduction

The scale-invariant ratio

$$h(\mathbf{x}) = \begin{cases} \frac{\|\mathbf{x}\|_1}{\|\mathbf{x}\|_2}, & \text{if } \mathbf{x} \neq \mathbf{0} \\ a, & \text{otherwise} \end{cases}, \quad a \in [0, 1] \quad (1.1)$$

has gained traction as a surrogate for the ℓ_0 penalty in sparse modeling because it promotes few nonzeros [1, 2] while remaining invariant under rescaling of \mathbf{x} . The same property that makes h attractive—its ratio form—also makes it non-convex and non-smooth, complicating both analysis and computation.

A central tool for optimization with nonsmooth terms is the proximity operator, see, [3–10] and the references therein. For a proper lower semicontinuous function f and a point \mathbf{y} , the proximity operator of f with parameter $\mu > 0$ denoted as $\text{prox}_{\mu f}(\mathbf{y})$, is defined as:

$$\text{prox}_{\mu f}(\mathbf{y}) = \arg \min_{\mathbf{x} \in \mathbb{R}^n} Q_{\mathbf{y}}(\mathbf{x}) := \frac{1}{2} \|\mathbf{x} - \mathbf{y}\|_2^2 + \mu f(\mathbf{x}). \quad (1.2)$$

In simpler terms, the proximity operator finds a point \mathbf{x} that minimizes the sum of the function f and half of the squared Euclidean distance between \mathbf{x} and a given point \mathbf{y} . There exists a rich class of efficient optimization algorithms based on the proximity operator including the primal-dual algorithm [6] and FISTA [11]. In other words, when a closed form (or an exact, low-cost procedure) is available, these methods become markedly simpler and more robust.

Two lines of work have addressed $\text{prox}_{\mu h}$ directly. The work in [12] derives a closed form under the assumption that the *true* sparsity (number of nonzeros of the proximal point) is known; in practice, a bisection heuristic is then used to guess this sparsity, which can introduce numerical errors or miss the optimal support. A second approach in [13] exploits the scale- and permutation-invariance of h to reformulate the task as a quadratic program on a portion of the sphere and solves it via projected gradient descent; however, the required projection is tractable only in low dimensions, limiting scalability. These limitations motivate a method that (i) avoids sparsity guessing, (ii) scales with dimension, and (iii) returns exact proximal solutions.

In this work, we adopt a manifold-optimization perspective that transforms $\text{prox}_{\mu h}(\mathbf{y})$ into a smooth problem on the unit sphere. The resulting structure reveals that any proximal point corresponds to a local, but non-global, minimizer of a quadratic objective restricted to the sphere; more specifically, solutions lie in a finite candidate set characterized via quartic polynomials. This characterization enables specialized procedures that compute those candidates exactly and select the true proximal solution. Unlike previous methods in [12, 13], our approach neither guesses sparsity nor depends on low-dimensional projections, and it can enumerate all proximal points when the prox is non-unique.

The paper is organized as follows. In [Section 2](#), we reformulate the computation of the proximity operator as a smooth manifold optimization problem. We then provide the characterizations of the proximity operator as local non-global minimizers of

certain quartic functions in [Section 3](#). Algorithms for computing the exact proximity operator have been developed in [Section 4](#). We further refine the optimization process in [Section 5](#) by analyzing the properties of these local non-global minimizers. Finally, we provide experimental results in [Section 6](#) to demonstrate the effectiveness of our approach.

2 Proximity operator via manifold optimization

In this section, we reformulate the computation of the proximity operator

$$\text{prox}_{\mu h}(\mathbf{y}),$$

of the ℓ_1 over ℓ_2 function h with parameter $\mu > 0$ at $\mathbf{y} \in \mathbb{R}^n$, as a smooth manifold optimization problem on a subset of the unit sphere.

First, recall that for any $\mathbf{x} \in \mathbb{R}^n$, we have $\|\mathbf{x}\|_2 \leq \|\mathbf{x}\|_1 \leq \sqrt{n}\|\mathbf{x}\|_2$. Since $a \in [0, 1]$ by assumption, it follows immediately that

$$\text{prox}_{\mu h}(\mathbf{0}) = \mathbf{0}.$$

Henceforth, we focus on the nontrivial case $\mathbf{y} \neq \mathbf{0}$.

The main difficulty in computing $\text{prox}_{\mu h}$ arises from the nonconvexity and the nonsmoothness of h . To address this, we follow the manifold optimization approach in [\[13\]](#). For any $\mathbf{x} \in \mathbb{R}^n \setminus \{\mathbf{0}\}$, we can represent it in polar form as

$$\mathbf{x} = r\mathbf{u}, \quad \text{for some } r \in \mathbb{R} \setminus \{0\} \text{ and } \mathbf{u} \in \mathbb{S}^{n-1}, \quad (2.1)$$

where $\mathbb{S}^{n-1} := \{\mathbf{u} \in \mathbb{R}^n : \|\mathbf{u}\|_2 = 1\}$ is the unit sphere in \mathbb{R}^n . Substituting (2.1) into the proximal objective for $h(\mathbf{x}) = \|\mathbf{x}\|_1/\|\mathbf{x}\|_2$ gives

$$\begin{aligned} Q_{\mathbf{y}}(\mathbf{x}) &= \frac{1}{2}\|\mathbf{y} - \mathbf{x}\|_2^2 + \mu h(\mathbf{x}) \\ &= \frac{1}{2}\|\mathbf{y} - r\mathbf{u}\|_2^2 + \mu \|\mathbf{u}\|_1 \\ &= \frac{1}{2}\|\mathbf{y}\|_2^2 + \frac{1}{2}(r - \langle \mathbf{y}, \mathbf{u} \rangle)^2 - \frac{1}{2}\langle \mathbf{y}, \mathbf{u} \rangle^2 + \mu \|\mathbf{u}\|_1, \end{aligned}$$

since $\|r\mathbf{u}\|_1/\|r\mathbf{u}\|_2 = \|\mathbf{u}\|_1$ when $\|\mathbf{u}\|_2 = 1$. For fixed \mathbf{u} , the minimizer with respect to r is immediate:

$$r = \langle \mathbf{y}, \mathbf{u} \rangle. \quad (2.2)$$

With (2.2) the problem (1.2) of minimizing $Q_{\mathbf{y}}$ reduces to an optimization over the sphere:

$$\mathbf{u}_{\mathbf{y}} = \arg \min_{\mathbf{u} \in \mathbb{S}^{n-1}} -\frac{1}{2}\langle \mathbf{y}, \mathbf{u} \rangle^2 + \mu \|\mathbf{u}\|_1. \quad (2.3)$$

Once \mathbf{u}_y is obtained, we recover the proximity operator by combining (2.1) and (2.2):

$$\text{prox}_{\mu h}(\mathbf{y}) = \begin{cases} \{\mathbf{0}\}, & \text{if } -\frac{1}{2}\langle \mathbf{y}, \mathbf{u}_y \rangle^2 + \mu \|\mathbf{u}_y\|_1 > \mu a; \\ \{\mathbf{0}, \langle \mathbf{y}, \mathbf{u}_y \rangle \mathbf{u}_y\}, & \text{if } -\frac{1}{2}\langle \mathbf{y}, \mathbf{u}_y \rangle^2 + \mu \|\mathbf{u}_y\|_1 = \mu a; \\ \{\langle \mathbf{y}, \mathbf{u}_y \rangle \mathbf{u}_y\}, & \text{if } -\frac{1}{2}\langle \mathbf{y}, \mathbf{u}_y \rangle^2 + \mu \|\mathbf{u}_y\|_1 < \mu a. \end{cases} \quad (2.4)$$

Equation (2.4) is a selection rule comparing the two only relevant candidates: the nonzero point $\langle \mathbf{y}, \mathbf{u}_y \rangle \mathbf{u}_y$ and the origin. Since $\frac{1}{2}\|\mathbf{y}\|_2^2$ cancels, the decision depends solely on $-\frac{1}{2}\langle \mathbf{y}, \mathbf{u}_y \rangle^2 + \mu \|\mathbf{u}_y\|_1$ and μa . Whichever objective value is smaller determines the proximal point; equality yields a set-valued prox.

The problem (2.3) remains unresolved due to the ℓ_1 term. However, we note that the minimizer \mathbf{u}_y must share the same sign pattern as \mathbf{y} . Therefore, replacing \mathbf{y} with its componentwise absolute value $|\mathbf{y}|$, we obtain a simple relation between the minimizers:

$$\mathbf{u}_y = \mathbf{u}_{|\mathbf{y}|} \odot \text{sign}(\mathbf{y}), \quad (2.5)$$

where \odot denotes componentwise multiplication and $\text{sign}(\mathbf{y})$ is the componentwise sign of \mathbf{y} .

Thus, it suffices to study the problem with $|\mathbf{y}|$, in which case the minimizer $\mathbf{u}_{|\mathbf{y}|}$ has nonnegative components. This observation allows us to replace the nonsmooth ℓ_1 -term by a linear one.

To formalize this, we introduce the following subsets of the unit sphere:

$$\begin{aligned} \mathbb{S}_+^{n-1} &= \{\mathbf{u} \in \mathbb{S}^{n-1} : u_i \geq 0, 1 \leq i \leq n\}, \\ \mathbb{S}_{++}^{n-1} &= \{\mathbf{u} \in \mathbb{S}^{n-1} : u_i > 0, 1 \leq i \leq n\}, \\ \mathbb{S}_-^{n-1} &= \{\mathbf{u} \in \mathbb{S}^{n-1} : u_i \leq 0, 1 \leq i \leq n\}. \end{aligned}$$

For convenience, we refer to these as the nonnegative orthant, positive orthant, and nonpositive orthant of the unit sphere, respectively.

For $\mathbf{x} \in \mathbb{R}^n$, define the smooth function

$$F_{\mathbf{y}}(\mathbf{u}) = -\frac{1}{2}\langle \mathbf{y}, \mathbf{u} \rangle^2 + \mu \langle \mathbf{1}_n, \mathbf{u} \rangle, \quad \mathbf{u} \in \mathbb{R}^n,$$

where $\mathbf{1}_n$ is the all-one vector in \mathbb{R}^n . Then we can rewrite the following.

$$\mathbf{u}_{|\mathbf{y}|} = \underset{\mathbf{u} \in \mathbb{S}_+^{n-1}}{\text{argmin}} F_{|\mathbf{y}|}(\mathbf{u}). \quad (2.6)$$

In summary, the nonsmooth and nonconvex problem defining $\text{prox}_{\mu h}(\mathbf{y})$ has been reformulated into the smooth quadratic optimization problem (2.6) over the nonnegative orthant of the unit sphere. Once $\mathbf{u}_{|\mathbf{y}|}$ is obtained, the proximity operator can be recovered via (2.4) and (2.5). In next section, we will characterize the solution $\mathbf{u}_{|\mathbf{y}|}$ and develop algorithms to compute it exactly.

3 Structural characterizations of the proximity operator

We now compute the minimizer $\mathbf{u}_{|\mathbf{y}|}$ of the function $F_{|\mathbf{y}|}$ in (2.6) through a structural characterization of its solutions. Specifically, we show that the solutions of (2.6) belong to a finite set of local non-global minimizers of certain quadratic functions. Based on this characterization, we will later introduce algorithms to compute these minimizers and identify the solution $\mathbf{u}_{|\mathbf{y}|}$ among them.

To proceed, we first sort the components of $|\mathbf{y}|$ in a non-increasing order. Specifically, for any $n \in \mathbb{N}$, we denote the set of vectors with non-increasing components as \mathbb{R}_+^n and let P be a permutation operator that sorts the components of $|\mathbf{y}|$ in a non-increasing order, and define

$$\mathbf{\eta} = \mathsf{P} |\mathbf{y}|.$$

After finding the solution $\mathbf{u}_{\mathbf{\eta}}$, we could obtain the solution $\mathbf{u}_{|\mathbf{y}|}$ by applying the inverse permutation operator P^{-1} to $\mathbf{u}_{\mathbf{\eta}}$:

$$\mathbf{u}_{|\mathbf{y}|} = \mathsf{P}^{-1} \mathbf{u}_{\mathbf{\eta}}. \quad (3.1)$$

We point out that the permutation operator P might not be unique since some components of $|\mathbf{y}|$ might be equal. In such cases, we arbitrarily fix one choice.

We next characterize $\mathbf{u}_{\mathbf{\eta}}$. If $\mathbf{\eta}$ has equal components, i.e., $\eta_i = \eta_j$ for some $1 \leq i < j \leq n$, then exchanging the corresponding entries of $\mathbf{u}_{\mathbf{\eta}}$ produces another minimizer. Such minimizers are regarded as equivalent. To eliminate ambiguity, we select as the canonical representative the minimizer satisfying $[\mathbf{u}_{\mathbf{\eta}}]_i \geq [\mathbf{u}_{\mathbf{\eta}}]_j$ whenever $\eta_i = \eta_j$. Other minimizers within the equivalence class are obtained by permuting the entries associated with equal components of $\mathbf{\eta}$. In the following, we restrict attention to this representation.

We first establish that the minimizer $\mathbf{u}_{\mathbf{\eta}}$ inherits the order of $\mathbf{\eta}$.

Lemma 3.1. *The minimizer $\mathbf{u}_{\mathbf{\eta}}$ of the function $F_{\mathbf{\eta}}$ in (2.6) belongs to \mathbb{R}_+^n .*

Proof For any $1 \leq i < j \leq n$, we need to show that $[\mathbf{u}_{\mathbf{\eta}}]_i \geq [\mathbf{u}_{\mathbf{\eta}}]_j$. Since $\mathbf{\eta} \in \mathbb{R}_+^n$, we have $\eta_i \geq \eta_j$. If $\eta_i = \eta_j$, by the definition of the representative of the equivalence class of minimizers, we have $[\mathbf{u}_{\mathbf{\eta}}]_i \geq [\mathbf{u}_{\mathbf{\eta}}]_j$. It remains to show it also holds when $\eta_i > \eta_j$. In this case, we can swap the components of $\mathbf{u}_{\mathbf{\eta}}$ corresponding to i and j to get a new vector $\mathbf{u}'_{\mathbf{\eta}}$. It follows that

$$\langle \mathbf{\eta}, \mathbf{u}_{\mathbf{\eta}} \rangle - \langle \mathbf{\eta}, \mathbf{u}'_{\mathbf{\eta}} \rangle = (\eta_i - \eta_j)([\mathbf{u}_{\mathbf{\eta}}]_i - [\mathbf{u}_{\mathbf{\eta}}]_j)$$

and $\langle \mathbf{1}_n, \mathbf{u}_{\mathbf{\eta}} \rangle = \langle \mathbf{1}_n, \mathbf{u}'_{\mathbf{\eta}} \rangle$. On the other hand, since $\mathbf{u}_{\mathbf{\eta}}$ is a minimizer of $F_{\mathbf{\eta}}$, we have $F_{\mathbf{\eta}}(\mathbf{u}_{\mathbf{\eta}}) \leq F_{\mathbf{\eta}}(\mathbf{u}'_{\mathbf{\eta}})$, which implies $\langle \mathbf{\eta}, \mathbf{u}_{\mathbf{\eta}} \rangle \geq \langle \mathbf{\eta}, \mathbf{u}'_{\mathbf{\eta}} \rangle$. When $\eta_i > \eta_j$, we also have $[\mathbf{u}_{\mathbf{\eta}}]_i \geq [\mathbf{u}_{\mathbf{\eta}}]_j$, which finishes the proof. \square

The above lemma provides a convenient way to find the minimizer \mathbf{u}_η . Since the components of \mathbf{u}_η are non-increasing, if one component of \mathbf{u}_η is zero, then all subsequent components must also be zero. Therefore, it suffices to determine the leading non-zero components of \mathbf{u}_η .

We will show that this leading non-zero subvector of \mathbf{u}_η is a local non-global minimizer of a quadratic function on the unit sphere. Existing results on minimizing quadratic functions on the unit sphere [14, 15] can then be applied to identify such minimizers.

To this end, we consider the following minimization problem on the unit sphere: for any $1 \leq k \leq n$,

$$\min_{\mathbf{u} \in \mathbb{S}^{k-1}} F_{\eta:k}(\mathbf{u}) = -\frac{1}{2} \mathbf{u}^\top \eta_{:k} (\eta_{:k})^\top \mathbf{u} + \mu \mathbf{u}^\top \mathbf{1}_k, \quad (3.2)$$

where $\eta_{:k} \in \mathbb{R}^k$ is the vector formed by the first k components of η . This formulation arises naturally: once we restrict \mathbf{u}_η to its first k coordinates, its norm constraint requires it to lie on the $(k-1)$ -dimensional unit sphere \mathbb{S}^{k-1} . The objective function then becomes quadratic in \mathbf{u} , with a rank-one negative semidefinite part and a linear bias term.

For each $1 \leq k \leq n$, we define the following set that may contain the true minimizer:

$$\mathcal{C}_k = \{ \mathbf{u} : \mathbf{u} \text{ is a local non-global minimizer of } F_{\eta:k} \text{ on } \mathbb{S}^{k-1} \text{ and } \mathbf{u} \in \mathbb{S}_{++}^{k-1} \} \quad (3.3)$$

and

$$\tilde{\mathcal{C}}_k = \{ (\mathbf{u}, \mathbf{0}_{n-k}) \in \mathbb{S}^{n-1} : \mathbf{u} \in \mathcal{C}_k \},$$

where $\mathbf{0}_{n-k}$ is the zero vector in \mathbb{R}^{n-k} . Intuitively, \mathcal{C}_k captures the possible active part of the minimizer in the first k coordinates, while $\tilde{\mathcal{C}}_k$ pads this solution with zeros to match the ambient dimension n .

It is known that a quadratic function on the unit sphere has at most one local-global minimizer [14]. Therefore, for each $1 \leq k \leq n$, the set \mathcal{C}_k is a singleton or empty, and the same holds for $\tilde{\mathcal{C}}_k$.

Therefore, the search for the minimizer \mathbf{u}_η reduces to checking finitely many candidate sets \mathcal{C}_k . Our subsequent analysis will show that the true minimizer must belong to one such set for some k . Intuitively, the choice of k corresponds to the active length of \mathbf{u}_η , i.e., how many of its leading coordinates remain nonzero before the sequence drops to zero.

We will show that the minimizer \mathbf{u}_η of F_η in (2.6) is in $\tilde{\mathcal{C}}_k$ for some $1 \leq k \leq n$.

Theorem 3.2. *The minimizer \mathbf{u}_η of the function F_η in (2.6) is in $\cup_{k=1}^n \tilde{\mathcal{C}}_k$. Specifically,*

$$\mathbf{u}_\eta = \arg \min_{\mathbf{u} \in \cup_{k=1}^n \tilde{\mathcal{C}}_k} F_\eta(\mathbf{u}). \quad (3.4)$$

Proof We will show that the minimizer \mathbf{u}_η of F_η in (2.6) is in $\tilde{\mathcal{C}}_k$ for some $1 \leq k \leq n$. By Lemma 3.1, \mathbf{u}_η is in \mathbb{R}_+^n . We also note that \mathbf{u}_η is in \mathbb{S}^{n-1} . It follows that we can write $\mathbf{u}_\eta = (\mathbf{u}, \mathbf{0}_{n-k})$ for some $1 \leq k \leq n$ and $\mathbf{u} \in \mathbb{S}_{++}^{k-1}$. It suffices to show that \mathbf{u} is a local non-global minimizer of $F_{\eta:k}$.

We first show that \mathbf{u} is a local minimizer of $F_{\eta:k}$ on \mathbb{S}^{k-1} . For any $\mathbf{u}' \in \mathbb{S}_{++}^{k-1}$, we have $(\mathbf{u}', \mathbf{0}_{n-k}) \in \mathbb{S}_+^{n-1}$. Since \mathbf{u}_η is a minimizer of F_η in (2.6), we have

$$F_\eta(\mathbf{u}_\eta) \leq F_\eta(\mathbf{u}').$$

On the other hand, we have $F_\eta(\mathbf{u}_\eta) = F_{\eta:k}(\mathbf{u})$ and $F_\eta(\mathbf{u}') = F_{\eta:k}(\mathbf{u}')$. Thus, we have

$$F_{\eta:k}(\mathbf{u}) \leq F_{\eta:k}(\mathbf{u}').$$

It holds for any $\mathbf{u}' \in \mathbb{S}_{++}^{k-1}$. Since \mathbb{S}_{++}^{k-1} is open in \mathbb{S}^{k-1} , we have \mathbf{u} is a local minimizer of $F_{\eta:k}$ on \mathbb{S}^{k-1} .

It remains to show that \mathbf{u} is not a global minimizer of $F_{\eta:k}$ on \mathbb{S}^{k-1} . It is direct to observe from the definition of $F_{\eta:k}$ in (3.2) that changing the sign of all positive components of \mathbf{u} to negative will yield a strictly smaller value of $F_{\eta:k}$. That is, the global minimizer of $F_{\eta:k}$ is in \mathbb{S}_-^{k-1} . Since \mathbb{S}_-^{k-1} is disjoint from \mathbb{S}_{++}^{k-1} , we have \mathbf{u} is not a global minimizer of $F_{\eta:k}$ on \mathbb{S}^{k-1} .

The specific form (3.4) of the minimizer \mathbf{u}_η follows immediately from the definition of \mathbf{u}_η . \square

We emphasize that the above theorem not only gives a characterization of the minimizer \mathbf{u}_η of F_η in (2.6), but also provides a way to find it. In particular, we can find all the local non-global minimizers of $F_{\eta:k}$ on \mathbb{S}^{k-1} for every $1 \leq k \leq n$ and then select the one with the smallest value of F_η . Moreover, for each $1 \leq k \leq n$, the set \mathcal{C}_k of local non-global minimizers is either empty or a singleton. That is, we are searching for the optimal one in a finite (at most n) set, which is guaranteed to have an exact solution.

We next show how to find \mathcal{C}_k and $\tilde{\mathcal{C}}_k$ through computing the local non-global minimizer of $F_{\eta:k}$ on \mathbb{S}^{k-1} for each $1 \leq k \leq n$.

When $k = 1$, $\mathbb{S}^0 = \{1, -1\}$. It is direct to see that the global minimizer is $\mathbf{u} = -1$ and the local non-global minimizer is $\mathbf{u} = 1$. That is, $\mathcal{C}_1 = \{1\}$.

For $k \geq 2$, we will use the method in [14] to find the local non-global minimizer of $F_{\eta:k}$ on \mathbb{S}^{k-1} . To this end, we will define the following quartic function: for any $2 \leq k \leq n$,

$$\psi_k(\lambda) := \sum_{i=0}^4 a_i \lambda^i, \quad (3.5)$$

where $a_0 = -\mu^2 \|\eta_{:k}\|_2^2 (k \|\eta_{:k}\|_2^2 - \|\eta_{:k}\|_1^2)$, $a_1 = 2\mu^2 (k \|\eta_{:k}\|_2^2 - \|\eta_{:k}\|_1^2)$, $a_2 = \|\eta_{:k}\|_2^4 - k\mu^2$, $a_3 = -2 \|\eta_{:k}\|_2^2$, and $a_4 = 1$. We will show that the local non-global minimizer of $F_{\eta:k}$ on \mathbb{S}^{k-1} depends on the roots of the above quartic function.

Theorem 3.3. *Suppose $2 \leq k \leq n$ and $\mathbf{u} \in \mathcal{C}_k$. Then*

- (i) *The quartic function ψ_k in (3.5) has (one or two distinct) real roots in $(\|\eta_{:k}\|_2^2 - \eta_k \|\eta_{:k}\|_1, \|\eta_{:k}\|_2^2)$.*

(ii) Let λ_k^* be the (larger one if we have two) root in (i). Then

$$\mathbf{u} = \frac{\mu}{\lambda_k^*(\|\mathbf{y}_{:k}\|_2^2 - \lambda_k^*)} \left[\|\mathbf{y}_{:k}\|_1 \mathbf{y}_{:k} - \left(\|\mathbf{y}_{:k}\|_2^2 - \lambda_k^* \right) \mathbf{1}_k \right]. \quad (3.6)$$

Proof We will use the result in [14] to characterize the local non-global minimizer \mathbf{u} . It has been shown in [14] that if \mathbf{s}^* is local non-global minimizer of the quadratic function $q(\mathbf{s}) = \frac{1}{2}\mathbf{s}^\top \mathbf{G}\mathbf{s} + \mathbf{g}^\top \mathbf{s}$ on the unit sphere \mathbb{S}^{k-1} , then

$$\mathbf{s}^* = -(\mathbf{G} + \lambda^* \mathbf{I}_k)^{-1} \mathbf{g}, \quad (3.7)$$

where λ^* is the larger root of $\varphi(\lambda) = 1$ in $(-\lambda_2, -\lambda_1)$ with $\varphi(\lambda) = \left\| (\mathbf{G} + \lambda \mathbf{I}_k)^{-1} \mathbf{g} \right\|_2^2$ and \mathbf{I}_k is the $k \times k$ identity matrix. Here, λ_1 and λ_2 are the two smallest eigenvalues of \mathbf{G} .

It is direct to observe from (3.2) that the quadratic function $F_{\mathbf{y}_{:k}}$ is in the form of $q(\mathbf{s})$ with $\mathbf{G} = -\mathbf{y}_{:k}(\mathbf{y}_{:k})^\top$ and $\mathbf{g} = \mu \mathbf{1}_k$. The two smallest eigenvalues of \mathbf{G} are $\lambda_1 = -\|\mathbf{y}_{:k}\|_2^2$ and $\lambda_2 = 0$. Moreover, we have

$$\varphi(\lambda) = \left\| (-\mathbf{y}_{:k}(\mathbf{y}_{:k})^\top + \lambda \mathbf{I}_k)^{-1} \mu \mathbf{1}_k \right\|^2.$$

By Sherman-Morrison formula [16], we have

$$(-\mathbf{y}_{:k}(\mathbf{y}_{:k})^\top + \lambda \mathbf{I}_k)^{-1} = \frac{1}{\lambda} \left(\mathbf{I}_k - \frac{1}{\lambda} \mathbf{y}_{:k}(\mathbf{y}_{:k})^\top \right)^{-1} = \frac{1}{\lambda} \left(\mathbf{I}_k - \frac{1}{\|\mathbf{y}_{:k}\|^2 - \lambda} \mathbf{y}_{:k}(\mathbf{y}_{:k})^\top \right). \quad (3.8)$$

It follows from a direct calculation that

$$\varphi(\lambda) = \frac{\mu^2}{\lambda^2} \left\| \mathbf{1}_k - \frac{\|\mathbf{y}_{:k}\|_1}{\|\mathbf{y}_{:k}\|^2 - \lambda} \mathbf{y}_{:k} \right\|^2 = 1 - \frac{\psi_k(\lambda)}{\lambda^2(\|\mathbf{y}_{:k}\|^2 - \lambda)^2}, \quad (3.9)$$

where $\psi_k(\lambda)$ is defined in (3.5). It implies λ^* is the larger root of $\psi_k(\lambda) = 0$ in $(0, \|\mathbf{y}_{:k}\|_2^2)$.

We next analyze the roots of $\psi_k(\lambda) = 0$. We observe that $\lim_{\lambda \rightarrow -\infty} \psi_k(\lambda) = \infty$ and $\psi_k(0) = a_0 = -\mu^2 \|\mathbf{y}_{:k}\|_2^2 (k \|\mathbf{y}_{:k}\|_2^2 - \|\mathbf{y}_{:k}\|_1^2) \leq 0$. Here we have used the fact that $\|\mathbf{y}_{:k}\|_1^2 \leq k \|\mathbf{y}_{:k}\|_2^2$ by Cauchy-Schwarz inequality. By Intermediate Value Theorem, ψ_k has a root in $(-\infty, 0]$. Similarly, we have $\lim_{\lambda \rightarrow \infty} \psi_k(\lambda) = \infty$ and $\psi_k(\|\mathbf{y}_{:k}\|_2^2) = -\mu^2 \|\mathbf{y}_{:k}\|_2^2 \|\mathbf{y}_{:k}\|_1^2 < 0$. It follows that ψ_k has a root in $(\|\mathbf{y}_{:k}\|_2^2, \infty)$. Thus, ψ_k has at most two distinct real roots in $(0, \|\mathbf{y}_{:k}\|_2^2)$. Let λ_k^* be the (larger one if we have two) root in $(0, \|\mathbf{y}_{:k}\|_2^2)$. It follows from (3.7) that

$$\mathbf{u} = -(-\mathbf{y}_{:k}(\mathbf{y}_{:k})^\top + \lambda_k^* \mathbf{I}_k)^{-1} \mu \mathbf{1}_k.$$

Substituting (3.8) into the above equation, we have

$$\mathbf{u} = \frac{\mu}{\lambda_k^*(\|\mathbf{y}_{:k}\|_2^2 - \lambda_k^*)} \left[\|\mathbf{y}_{:k}\|_1 \mathbf{y}_{:k} - (\|\mathbf{y}_{:k}\|_2^2 - \lambda_k^*) \mathbf{1}_k \right].$$

Since $\mathbf{u} \in \mathcal{C}_k$, we have $\mathbf{u} \in \mathbb{S}_{++}^{k-1}$ by the definition of \mathcal{C}_k in (3.3). It implies $\|\mathbf{y}_{:k}\|_1 \mathbf{y}_{:k} - (\|\mathbf{y}_{:k}\|_2^2 - \lambda_k^*) > 0$. Thus, we have $\lambda_k^* > \|\mathbf{y}_{:k}\|_2^2 - \|\mathbf{y}_{:k}\|_1$, which finishes the proof. \square

We remark that the quartic function ψ_k in (3.5) is a polynomial of degree 4 with real coefficients. Its roots have closed form solutions [17]. In the simplicity of presentation, we will not give the explicit form of the roots since its formula is complicated. Instead, we will present an example to demonstrate the calculation for a special case when all the components of $\mathbf{y}_{:k}$ are equal.

Example 3.4. Suppose $\mathbf{y}_{:k} = y \mathbf{1}_k$ for some $y > 0$. Then we have

$$a_0 = 0, a_1 = 0, a_2 = k^2 y^4 - k\mu^2, a_3 = -2ky^2, a_4 = 1.$$

The quartic function ψ_k in (3.5) has the following form:

$$\psi_k(\lambda) = \lambda^2((\lambda - ky^2)^2 - k\mu^2).$$

It has roots at $\lambda = 0$, $\lambda = ky^2 - \sqrt{k}\mu$, and $\lambda = ky^2 + \sqrt{k}\mu$. We need to find the larger root in $(\|\mathbf{y}_{:k}\|_2^2 - \mathbf{y}_{:k} \|\mathbf{y}_{:k}\|_1, \|\mathbf{y}_{:k}\|_2^2) = (0, ky^2)$. It is direct to see only when $\mu < y^2\sqrt{k}$, we have $\lambda_k^* = ky^2 - \sqrt{k}\mu$ and the optimal solution is given by:

$$\mathbf{u} = \frac{1}{\sqrt{k}} \mathbf{1}_k.$$

Otherwise, there is no local non-global minimizer in \mathbb{S}_{++}^{k-1} and $\mathcal{C}_k = \emptyset$.

We emphasize that Theorems 3.2 and 3.3 provide a specific way to compute the minimizer \mathbf{u}_η exactly. In particular, Theorem 3.3 shows how to find the set \mathcal{C}_k and $\tilde{\mathcal{C}}_k$ (either empty or a singleton) for each $1 \leq k \leq n$. Theorem 3.2 tells us to search for the optimal ones in a finite (at most n) set $\bigcup_{k=1}^n \tilde{\mathcal{C}}_k$, which has exact solutions. Moreover, the optimal solution \mathbf{u}_η might not be unique as shown in [12]. Our method can find all of them since we are searching in a finite set. After finding the minimizer \mathbf{u}_η , we can substitute it into (2.4), (2.5) and (3.1) to get the proximity operator $\text{prox}_{\mu h}(\mathbf{y})$ immediately:

$$\text{prox}_{\mu h}(\mathbf{y}) = \begin{cases} \{\mathbf{0}\}, & \text{if } -\frac{1}{2}\langle \mathbf{y}, \mathbf{u}_\eta \rangle^2 + \mu \|\mathbf{u}_\eta\|_1 > \mu a; \\ \{\mathbf{0}, \langle \mathbf{y}, \mathbf{P}^{-1}\mathbf{u}_\eta \odot \text{sign}(\mathbf{y}) \rangle (\mathbf{P}^{-1}\mathbf{u}_\eta \odot \text{sign}(\mathbf{y}))\}, & \text{if } -\frac{1}{2}\langle \mathbf{y}, \mathbf{u}_\eta \rangle^2 + \mu \|\mathbf{u}_\eta\|_1 = \mu a; \\ \{\langle \mathbf{y}, \mathbf{P}^{-1}\mathbf{u}_\eta \odot \text{sign}(\mathbf{y}) \rangle (\mathbf{P}^{-1}\mathbf{u}_\eta \odot \text{sign}(\mathbf{y}))\}, & \text{if } -\frac{1}{2}\langle \mathbf{y}, \mathbf{u}_\eta \rangle^2 + \mu \|\mathbf{u}_\eta\|_1 < \mu a. \end{cases} \quad (3.10)$$

4 Algorithm to compute the exact proximity operator

The characterizations in Theorems 3.2 and 3.3 suggest a direct procedure for computing the exact proximity operator $\text{prox}_{\mu h}(\mathbf{y})$. For each $1 \leq k \leq n$, we determine the candidate set \mathcal{C}_k (and its padded version $\tilde{\mathcal{C}}_k$ via Theorem 3.3; we then compare F_η on the finite union $\bigcup_{k=1}^n \tilde{\mathcal{C}}_k$ and select a minimizer \mathbf{u}_η of (2.3). Substituting \mathbf{u}_η into (3.10) yields $\text{prox}_{\mu h}(\mathbf{y})$. We summarize the above procedure in Algorithm 1.

Algorithm 1 Exact computation of the proximity operator $\text{prox}_{\mu h}(\mathbf{y})$ (naive).

Input: $\mathbf{y} \in \mathbb{R}^n$, $\mu > 0$
Output: $\text{prox}_{\mu h}(\mathbf{y})$

- 1: **if** $\mathbf{y} = \mathbf{0}$ **then**
- 2: **return** $\mathbf{0}$
- 3: **end if**
- 4: Sort the components of $|\mathbf{y}|$ in non-increasing order: find a permutation operator P such that $\mathbf{y} = P(|\mathbf{y}|) \in \mathbb{R}^n$.
- 5: Let $\mathcal{C}_1 = \{(1)\}$ and $\tilde{\mathcal{C}}_1 = \{(1, \mathbf{0}_{n-1})\}$.
- 6: **for** $k = 2, \dots$, **do**
- 7: Compute the coefficients a_0, a_1, a_2, a_3, a_4 of the quartic function ψ_k in (3.5) using \mathbf{y} .
- 8: Find the roots of $\psi_k(\lambda)$.
- 9: **if** there are roots in $(\|\mathbf{y}_{:k}\|_2^2 - \mathbf{y}_k \|\mathbf{y}_{:k}\|_1, \|\mathbf{y}_{:k}\|_2^2)$ **then**
- 10: Let λ_k^* be the larger root.
- 11: Compute the local non-global minimizer \mathbf{u} using (3.6).
- 12: Set $\mathcal{C}_k = \{\mathbf{u}\}$ and $\tilde{\mathcal{C}}_k = \{(\mathbf{u}, \mathbf{0}_{n-k})\}$.
- 13: **else**
- 14: Set $\mathcal{C}_k = \emptyset$ and $\tilde{\mathcal{C}}_k = \emptyset$.
- 15: **end if**
- 16: **end for**
- 17: Find the minimizer(s) \mathbf{u}_η of F_η in $\cup_{k=1}^n \tilde{\mathcal{C}}_k$ through comparing the values of F_η evaluated at the finite set $\cup_{k=1}^n \tilde{\mathcal{C}}_k$.
- 18: **return** the proximity operator $\text{prox}_{\mu h}(\mathbf{y})$ using (3.10).

We point out that the $\text{prox}_{\mu h}(\mathbf{y})$ might not be unique, as shown in [12]. Our method can find all of them since we are searching in a finite set.

The direct computational complexity of the above algorithm is $O(n^2)$. For each $2 \leq k \leq n$ in the iteration, computing the coefficients a_0, a_1, a_2, a_3, a_4 of the quartic function ψ_k in (3.5) takes $O(k)$ time. Finding the roots of the quartic function ψ_k takes $O(1)$ time and computing the local non-global minimizer \mathbf{u} using (3.6) takes $O(k)$ time. Moreover, the evaluation of F_η at each element in $\tilde{\mathcal{C}}_k$ takes $O(n)$ time. Since there are at most n elements in $\tilde{\mathcal{C}}_k$, the computational complexity of finding the smallest one is $O(n^2)$. Consequently, the total computational complexity of the above algorithm is $O(n^2)$.

However, we note that the computational complexity of finding the local non-global minimizers \mathcal{C}_k and finding the minimizer \mathbf{u}_η through comparing the values of F_η in $\cup_{k=1}^n \tilde{\mathcal{C}}_k$ could be reduced to $O(n)$. In particular, the coefficients of the quartic function in the above algorithm depends on $\|\mathbf{y}\|_2^2$ and $\|\mathbf{y}\|_1$. They could be computed in $O(n)$ time through the incremental manner. The evaluation of F_η at each local non-global minimizer \mathbf{u} in $\tilde{\mathcal{C}}_k$ could also be computed in the same way. To this end, we derive the specific calculation of F_η at elements in $\tilde{\mathcal{C}}_k$. For any $2 \leq k \leq n$ and $\bar{\mathbf{u}} \in \tilde{\mathcal{C}}_k$, there

exists a $\mathbf{u} \in \mathcal{C}_k$ such that $\bar{\mathbf{u}} = (\mathbf{u}, \mathbf{0}_{n-k})$. We have

$$F_{\mathbf{y}}(\bar{\mathbf{u}}) = -\frac{1}{2}(\mathbf{u}^T \mathbf{y}_{:k})^2 + \mu \mathbf{u}^T \mathbf{1}_k.$$

Substituting \mathbf{u} in (3.6) into the above equation gives for any $2 \leq k \leq n$ and $\bar{\mathbf{u}} \in \tilde{\mathcal{C}}_k$:

$$F_{\mathbf{y}}(\bar{\mathbf{u}}) = -\frac{1}{2} \frac{\mu^2 \|\mathbf{y}_{:k}\|_1^2}{(\|\mathbf{y}_{:k}\|_2^2 - \lambda_k^*)^2} + \frac{\mu^2}{\lambda_k^*(\|\mathbf{y}_{:k}\|_2^2 - \lambda_k^*)} \left(\|\mathbf{y}_{:k}\|_1^2 - k(\|\mathbf{y}_{:k}\|_2^2 - \lambda_k^*) \right). \quad (4.1)$$

We see that it is an $O(1)$ calculation given λ_k^* , $\|\mathbf{y}_{:k}\|_1$, and $\|\mathbf{y}_{:k}\|_2^2$. Since there are at most n elements in $\tilde{\mathcal{C}}_k$, the computational complexity of computing all the values of $F_{\mathbf{y}}$ at elements in $\tilde{\mathcal{C}}_k$ and finding the smallest one could be reduced to $O(n)$. We summarize the above optimized version in [Algorithm 2](#).

Algorithm 2 Exact computation of the proximity operator $\text{prox}_{\mu h}(\mathbf{y})$ (optimized).

Input: $\mathbf{y} \in \mathbb{R}^n$, $\mu > 0$
Output: $\text{prox}_{\mu h}(\mathbf{y})$, where $h(\mathbf{x}) = \mu \frac{\|\mathbf{x}\|_1}{\|\mathbf{x}\|_2}$.

- 1: **if** $\mathbf{y} = \mathbf{0}$ **then**
- 2: **return** $\mathbf{0}$
- 3: **end if**
- 4: Sort the components of $|\mathbf{y}|$ in non-increasing order: find a permutation operator P such that $\mathbf{y} = P(|\mathbf{y}|) \in \mathbb{R}_+^n$.
- 5: **Initialize:** $\tilde{\mathcal{C}} = \{(1, \mathbf{0}_{n-1})\}$, $S_1 = \mathbf{y}_1$, $S_2 = (\mathbf{y}_1)^2$, $\min_F = -\frac{1}{2}S_2 + \mu$
- 6: **for** $k = 2, \dots, n$ **do**
- 7: Update $S_1 = S_1 + \mathbf{y}_k$ and $S_2 = S_2 + (\mathbf{y}_k)^2$.
- 8: Compute a_0, a_1, a_2, a_3, a_4 of the quartic function ψ_k in (3.5) using S_1 and S_2 :

$$a_0 = -\mu^2 S_2 (kS_2 - S_1^2), a_1 = 2\mu^2 (kS_2 - S_1^2), a_2 = S_2^2 - k\mu^2, a_3 = -2S_2, a_4 = 1.$$

- 9: Find the roots of the quartic function.
- 10: **if** there are roots in $(S_2 - \mathbf{y}_k S_1, S_2)$ **then**
- 11: Let λ_k^* be the larger root.
- 12: Compute \mathbf{u} through substituting λ_k^* , S_1 , and S_2 into (3.6).
- 13: Compute $F_{\mathbf{y}}(\bar{\mathbf{u}})$ through substituting λ_k^* , S_1 , and S_2 into (4.1).
- 14: **if** $F_{\mathbf{y}}(\bar{\mathbf{u}}) < \min_F$ **then**
- 15: $\tilde{\mathcal{C}} = \{\bar{\mathbf{u}}\}$ and $\min_F = F_{\mathbf{y}}(\bar{\mathbf{u}})$
- 16: **else if** $F_{\mathbf{y}}(\bar{\mathbf{u}}) = \min_F$ **then**
- 17: $\tilde{\mathcal{C}} = \tilde{\mathcal{C}} \cup \{\bar{\mathbf{u}}\}$
- 18: **end if**
- 19: **end if**
- 20: **end for**
- 21: **return** $\text{prox}_{\mu h}(\mathbf{y})$ by substituting each $\mathbf{u}_{\mathbf{y}} \in \tilde{\mathcal{C}}$ into (3.10).

It is direct to see that every iteration of k in the above algorithm takes $O(1)$ time. The computational complexity of all the iterations is $O(n)$, which is much lower than the $O(n^2)$ complexity of the original [Algorithm 1](#).

5 Further improvements

The main idea of the proposed algorithms is to characterize the minimizer(s) of $F_{\mathbf{y}}$ through the local non-global minimizers of quadratic functions on unit sphere. In particular, we show that they are in a finite set $\cup_{k=1}^n \tilde{\mathcal{C}}_k$. That is, the optimization problem on an infinite set is reduced to a finite set. We can then search for the minimizer(s) in the finite set through direct comparison. However, we still need to find the roots of the quartic function ψ_k for each $1 \leq k \leq n$. We will show that we can further reduce the computational complexity by exploiting the properties of the local non-global minimizers.

We next present a necessary and sufficient condition for the existence of local non-global minimizers of $F_{\mathbf{y}_{:k}}$, allowing us to skip quartic solves whenever no such minimizer can exist; this yields a pruned variant that preserves exactness while further reducing work.

For each $2 \leq k \leq n$, recall the sphere problem

$$\min_{\mathbf{u} \in \mathbb{S}^{k-1}} F_{\mathbf{y}_k}(\mathbf{u}) = -\frac{1}{2} \mathbf{u}^\top \mathbf{y}_k (\mathbf{y}_k)^\top \mathbf{u} + \mu \mathbf{u}^\top \mathbf{1}_k,$$

and the candidate set \mathcal{C}_k of its local non-global minimizers in \mathbb{S}_{++}^{k-1} , with $\tilde{\mathcal{C}}_k = \{(\mathbf{u}, 0_{n-k}) : \mathbf{u} \in \mathcal{C}_k\}$. Define the prefix sums $S_1(k) = \|\mathbf{y}_k\|_1$ and $S_2(k) = \|\mathbf{y}_k\|_2^2$, and set

$$A_k := \left((k S_2(k) - S_1(k)^2)^{1/3} + S_1(k)^{2/3} \right) S_2(k)^{-1}. \quad (5.1)$$

The following condition exactly characterizes the k for which $\mathcal{C}_k \neq \emptyset$.

Theorem 5.1. *For each $2 \leq k \leq n$, the set \mathcal{C}_k is nonempty if and only if*

$$A_k \leq \mu^{-\frac{2}{3}}. \quad (5.2)$$

Proof From [Theorem 3.3](#), we know that for each $2 \leq k \leq n$, the local non-global minimizer of $F_{\mathbf{y}_{:k}}$ exists if and only if $\varphi(\lambda) = 1$ has a root in $(0, \|\mathbf{y}_{:k}\|_2^2)$, where $\varphi(\lambda)$ is defined in [\(3.9\)](#). We will prove the desired result through analyzing the behavior of $\varphi(\lambda)$ in this interval.

We first rewrite $\varphi(\lambda)$ in [\(3.9\)](#) as

$$\begin{aligned} \varphi(\lambda) &= \frac{\mu^2}{\lambda^2} \left(k + \frac{\|\mathbf{y}_{:k}\|_1^2 (2\lambda - \|\mathbf{y}_{:k}\|_2^2)}{(\|\mathbf{y}_{:k}\|_2^2 - \lambda)^2} \right) \\ &= \mu^2 \left(k\lambda^{-2} + \|\mathbf{y}_{:k}\|_1^2 \left(\frac{1}{\lambda(\|\mathbf{y}_{:k}\|_2^2 - \lambda)^2} - \frac{1}{\lambda^2(\|\mathbf{y}_{:k}\|_2^2 - \lambda)} \right) \right). \end{aligned}$$

Its derivative is given by

$$\varphi'(\lambda) = 2\mu^2 \left(-k\lambda^{-3} + \|\mathbf{y}_{:k}\|_1^2 \lambda^{-3} (\|\mathbf{y}_{:k}\|_2^2 - \lambda)^{-3} \left(\lambda^2 - \lambda(\|\mathbf{y}_{:k}\|_2^2 - \lambda) + (\|\mathbf{y}_{:k}\|_2^2 - \lambda)^2 \right) \right)$$

$$\begin{aligned}
&= 2\mu^2 \left(-k\lambda^{-3} + \|\mathbf{y}_{:k}\|_1^2 \lambda^{-3} (\|\mathbf{y}_{:k}\|_2^2 - \lambda)^{-3} \frac{\lambda^3 + (\|\mathbf{y}_{:k}\|_2^2 - \lambda)^3}{\lambda + \|\mathbf{y}_{:k}\|_2^2 - \lambda} \right) \\
&= \frac{2\mu^2}{\|\mathbf{y}_{:k}\|_2^2} \left(\|\mathbf{y}_{:k}\|_1^2 (\|\mathbf{y}_{:k}\|_2^2 - \lambda)^{-3} - (k \|\mathbf{y}_{:k}\|_2^2 - \|\mathbf{y}_{:k}\|_1^2) \lambda^{-3} \right)
\end{aligned}$$

and its second derivative is

$$\varphi''(\lambda) = \frac{6\mu^2}{\|\mathbf{y}_{:k}\|_2^2} \left(\|\mathbf{y}_{:k}\|_1^2 (\|\mathbf{y}_{:k}\|_2^2 - \lambda)^{-4} + (k \|\mathbf{y}_{:k}\|_2^2 - \|\mathbf{y}_{:k}\|_1^2) \lambda^{-4} \right).$$

We point out that the special case when $\mathbf{y}_{:k} = \mathbf{y}_1 \mathbf{1}_k$ has already been discussed in [Example 3.4](#). That is, the local non-global minimizer of $F_{\mathbf{y}_{:k}}$ exists if and only if

$$\mu < (\mathbf{y}_1)^2 \sqrt{k}.$$

It is direct to observe that the above inequality is equivalent to the condition in [\(5.2\)](#) for this special case.

It remains to analyze the case when $\mathbf{y}_{:k} \neq \mathbf{y}_1 \mathbf{1}_k$. We observe that $\lim_{\lambda \rightarrow 0^+} \varphi(\lambda) = \lim_{\lambda \rightarrow (\|\mathbf{y}_{:k}\|_2^2)^-} \varphi(\lambda) = \infty$, which implies that $\varphi(\lambda) = 1$ has a root in $(0, \|\mathbf{y}_{:k}\|_2^2)$ if and only if the minimum value of $\varphi(\lambda)$ on $(0, \|\mathbf{y}_{:k}\|_2^2)$ is less than or equal to 1. When $\mathbf{y}_{:k} \neq \mathbf{y}_1 \mathbf{1}_k$, we have $k \|\mathbf{y}_{:k}\|_2^2 - \|\mathbf{y}_{:k}\|_1^2 > 0$. It implies $\varphi''(\lambda) > 0$ for all $\lambda \in (0, \|\mathbf{y}_{:k}\|_2^2)$ and $\varphi'(\lambda) = 0$ has a unique solution in $(0, \|\mathbf{y}_{:k}\|_2^2)$:

$$\lambda_0 = \frac{\|\mathbf{y}_{:k}\|_2^2}{1 + \left(\frac{\|\mathbf{y}_{:k}\|_1^2}{k \|\mathbf{y}_{:k}\|_2^2 - \|\mathbf{y}_{:k}\|_1^2} \right)^{\frac{1}{3}}}.$$

That is, the minimum value of $\varphi(\lambda)$ on $(0, \|\mathbf{y}_{:k}\|_2^2)$ is given by $\varphi(\lambda_0)$. Thus, the local non-global minimizer of $F_{\mathbf{y}_{:k}}$ exists if and only if $\varphi(\lambda_0) \leq 1$. Substituting $\lambda = \lambda_0$ into $\varphi(\lambda)$, we get:

$$\varphi(\lambda_0) = \mu^2 \left(\frac{(k \|\mathbf{y}_{:k}\|_2^2 - \|\mathbf{y}_{:k}\|_1^2)^{\frac{1}{3}} + \|\mathbf{y}_{:k}\|_1^{\frac{2}{3}}}{\|\mathbf{y}_{:k}\|_2^2} \right)^3 = \mu^2 A_k^3.$$

The desired condition [\(5.2\)](#) is equivalent to $\varphi(\lambda_0) \leq 1$, which gives us the necessary condition for the existence of a local non-global minimizer. \square

We emphasize that the above theorem provides a necessary and sufficient condition for the existence of local non-global minimizers of $F_{\mathbf{y}_{:k}}$. It suggests that we might not need to find the roots of the quartic function ψ_k in [\(3.5\)](#) for all $2 \leq k \leq n$. Instead, we can first check whether the condition in [\(5.2\)](#) holds. If it does, we then find the roots of ψ_k to get the local non-global minimizer. Otherwise, we set $\mathcal{C}_k = \emptyset$ and $\tilde{\mathcal{C}}_k = \emptyset$. This will further reduce the computational complexity of [Algorithm 2](#).

One may wonder whether the condition in [\(5.2\)](#) can help us to determine the range of k such that the local non-global minimizers of $F_{\mathbf{y}_{:k}}$ exist. That is, if the condition in [\(5.2\)](#) fails at some k_0 , does it fail for all $k > k_0$? Could we find an interval (k_0, k_1) such that the condition holds for all $k \in (k_0, k_1)$? In this case, we could use techniques such as bisection method to locate such an interval and might not need to check it for every k in $[2, n]$. Unfortunately, we find that this is not true through some numerical experiments. In particular, we find that the condition in [\(5.2\)](#) may hold for some k ,

fail for some $k > k_0$, and then hold again for some $k > k_1$. Thus, we still need to check the condition in (5.2) for each $2 \leq k \leq n$ in our algorithms.

The following example shows a case when the quantity A_k in (5.2) has a “zig-zag” behavior.

Example 5.2. Let $\mathbf{y} = [1, 1, 0.92, 0.92, 0.8, 0.8, 0.8, 0.5]^\top$. The values of A_k (5.1) for $2 \leq k \leq 8$ are given in Figure 1. We see that A_k has a zig-zag behavior.

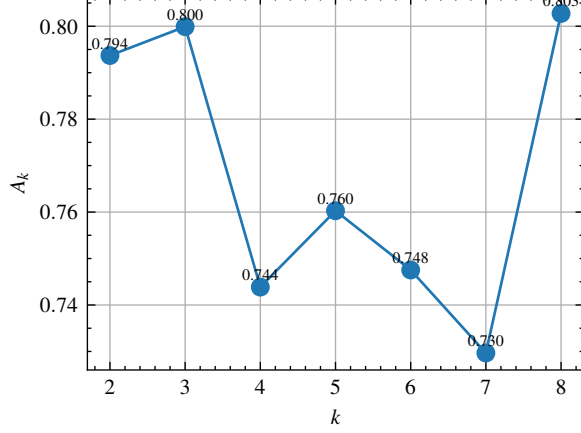


Fig. 1: The values of A_k (5.1) for $2 \leq k \leq 8$.

It is direct to observe that when choosing $\mu^{-\frac{2}{3}} = 0.795$, the condition (5.2) holds for $k = 2, 4, 5, 6, 7$, but fails for $k = 3, 8$. When choosing $\mu^{-\frac{2}{3}} = 0.755$, the condition (5.2) holds for $k = 4, 6, 7$, but fails for $k = 2, 3, 5, 8$.

Another interesting question is whether we can find a monotone pattern of the function value $F_{\mathbf{y}}(\bar{\mathbf{u}}_k)$ corresponding to local non-global minimizers $\mathbf{u}_k \in \mathcal{C}_k$. If it is true, we might not need to compare the values of $F_{\mathbf{y}}$ at all the local non-global minimizers. Instead, we can find the smallest one through some efficient search method. Unfortunately, we find that this is not true either through some numerical experiments.

Example 5.3. We consider $\mathbf{y} = [42, 26.52, 2.39, 2.247, 1.923, 1.849, 1.150, 0.634, 0.073]^\top$ and $\mu = 0.0001$. The local non-global minimizers of $F_{\mathbf{y},k}$ exist for $1 \leq k \leq 9$. The corresponding function values $F_{\mathbf{y}}(\bar{\mathbf{u}}_k)$ are given in Figure 2. We see that the function values do not have a monotone pattern.

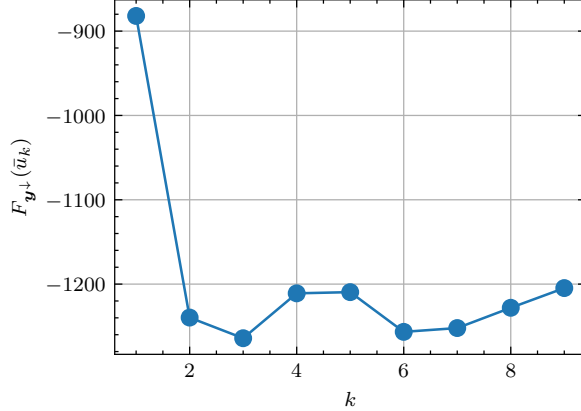


Fig. 2: The function values $F_{y^k}(\bar{u}_k)$ for $1 \leq k \leq 9$.

6 Numerical experiments

We will present some numerical experiments to illustrate the performance of our proposed algorithms. In particular, we will compare the performance of our algorithms with the algorithm proposed in [12]. To align with that baseline, we set the value at the origin to $a = 1$ in (1.1). Across all tested problems, our algorithms return the exact proximal solution, whereas the algorithm of [12] fails to reach the exact solution on certain inputs.

We point out that the algorithm in [12] is designed for solving the proximity operator with the original objective function $Q_{\mathbf{y}}$ in (1.2) directly. We will also display our results in terms of the function values of $Q_{\mathbf{y}}$ in the convenience of comparison. To this end, for every local non-global minimizer \mathbf{u}_k of F_{y^k} , we compute the corresponding value of \mathbf{x} as

$$\mathbf{x}_k = \mathsf{P}^{-1} \bar{\mathbf{u}}_k \langle \bar{\mathbf{u}}_k, \mathbf{y} \rangle$$

and evaluate the function value $Q_{\mathbf{y}}(\mathbf{x}_k)$. Note that the solution of the proximity operator $\text{prox}_h^\mu(\mathbf{y})$ is the \mathbf{x}_k that gives the smallest function value $Q_{\mathbf{y}}(\mathbf{x}_k)$ among all k such that the local non-global minimizers of F_{y^k} exist.

Example 6.1. Consider the vector $\mathbf{y} = [4, 4, 3, 3, 2, 2]$ with parameter $\mu = 1$ and $\mu = 13$. For both cases, local non-global minimizers of F_{y^k} are present for all k from 1 to 6. The plots in Figure 3 illustrate the function values $Q_{\mathbf{y}}(\mathbf{x}_k)$ across these values of k .

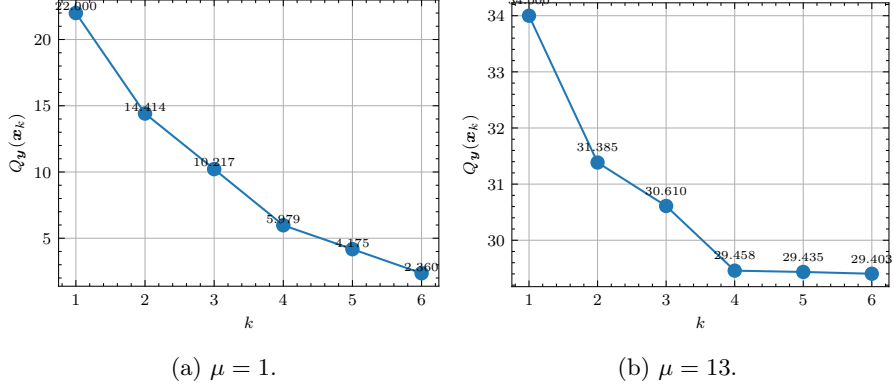


Fig. 3: Function values $Q_{\mathbf{y}}(\mathbf{x}_k)$ in [Example 6.1](#).

The table below summarizes the sparsity level k , the computed proximity operator $\text{prox}_{\mu h}(\mathbf{y})$, and the corresponding function value $Q_{\mathbf{y}}(\text{prox}_h^{\mu}(\mathbf{y}))$ for both algorithms.

μ	Algorithm	Sparsity level k	$\text{prox}_h^{\mu}(\mathbf{y})$	$Q_{\mathbf{y}}(\text{prox}_h^{\mu}(\mathbf{y}))$
1	Proposed [12]	6	$[4.033, 4.033, 2.990, 2.990, 1.948, 1.948]^T$	2.360
		6	$[4.033, 4.033, 2.990, 2.990, 1.948, 1.948]^T$	2.360
13	Proposed [12]	6	$[4.455, 4.455, 2.423, 2.423, 0.392, 0.392]^T$	29.403
		3	$[3.597, 3.597, 1.542, 0, 0, 0]^T$	31.091

Table 1: Comparison of the two algorithms for [Example 6.1](#).

When $\mu = 1$, both our proposed method and the method from [12] select $k = 6$, yielding the same solution with a function value of 2.360.

However, when $\mu = 13$, the two methods yield different results. The minimum function value, 29.403, is achieved at $k = 6$ by our proposed method. In contrast, the approach from [12] selects $k = 3$, resulting in a higher function value of 31.091. This demonstrates that our method identifies the true optimal solution, while the method in [12] does not always do so. Even when both methods select the same sparsity level $k = 3$, our method yields a superior solution with a lower function value of 30.610 compared to 31.091 from [12].

Example 6.2. We consider $\mathbf{y} = [9, 7, 6, 4, 2]^T$ with $\mu = 1$ and $\mu = 48$. The local non-global minimizers of $F_{\mathbf{y}, k}$ exist for $1 \leq k \leq 5$ with $\mu = 1$ and exist for $1 \leq k \leq 4$ with $\mu = 48$. We plot the function values $Q_{\mathbf{y}}(\mathbf{x}_k)$ in [Figure 4](#).

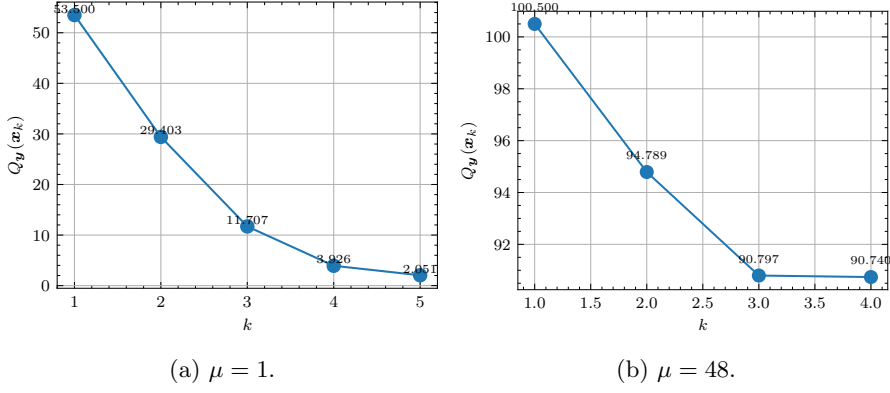


Fig. 4: Function values $Q_y(x_k)$ in Example 6.2.

We display the solutions of the sparsity level k , the proximity operator $\text{prox}_{\mu h}(\mathbf{y})$, and the corresponding function values $Q_y(\text{prox}_{\mu h}(\mathbf{y}))$ for the two algorithms in Table 2.

μ	Algorithm	Sparsity level k	$\text{prox}_{\mu h}(\mathbf{y})$	$Q_y(\text{prox}_{\mu h}(\mathbf{y}))$
1	Proposed [12]	5	$[9.026, 7.004, 5.993, 3.970, 1.948]^\top$	2.051
		4	$[9.021, 7.000, 5.989, 3.968, 0]^\top$	3.926
48	Proposed [12]	4	$[10.255, 6.362, 4.415, 0.521, 0]^\top$	90.740
		2	$[8.506, 4.642, 0, 0, 0]^\top$	96.030

Table 2: Comparison of the two algorithms for Example 6.2.

When $\mu = 1$, our proposed method selects $k = 5$ and achieves a function value of 2.051, while the method from [12] selects $k = 4$ with a higher function value of 3.926. This indicates that our method finds the exact solution, whereas the method in [12] does not always do so.

When $\mu = 48$, we see that the smallest function value 90.740 of $Q_y(x_k)$ is attained at $k = 4$. However, the algorithm in [12] returns a solution with $k = 2$ and the function value 96.030. We see that our algorithm finds the exact solution, while the algorithm in [12] fails to find the exact solution. Moreover, even at the same sparsity level $k = 2$, our algorithm finds a better solution with a smaller function value 94.789 than 96.030 found in the algorithm [12].

We observe that the proposed algorithm consistently identifies the exact solution, while the method from [12] may not always achieve this. This discrepancy likely arises because the algorithm in [12] needs to use a heuristic bisection approach to determine the sparsity level k , which might lead to numerical inaccuracies or suboptimal choices. Moreover, even when both algorithms use the same sparsity level k , our method tends to find a solution with a lower function value, indicating a more optimal solution

within that sparsity constraint. In contrast, our algorithm systematically reduces the solution space to a finite number of candidates and is guaranteed to find the exact solution among these candidates.

7 Conclusion

We presented an exact and efficient framework for computing the proximity operator of the ratio $\|\mathbf{x}\|_1/\|\mathbf{x}\|_2$. By recasting the problem into radius–direction variables and working on the unit sphere, we proved that all proximal points arise from a finite family of local (but non-global) minimizers of a rank-one quadratic, characterized through the roots of an explicit quartic. This structure leads to a complete selection rule, a necessary and sufficient existence test for candidates, and practical algorithms—including a $O(n)$ implementation based on prefix sums—that return the exact proximal solution without guessing the support. Numerical experiments confirm exactness and show consistent improvements over a state-of-the-art baseline that can miss the optimum.

Acknowledgement

We are grateful to Dr. Min Tao for generously sharing the code accompanying [12], which facilitated our comparisons. The work of L. Shen was supported in part by the National Science Foundation under grant DMS-2208385. The work of G. Song was supported in part by the National Science Foundation under grant DMS-2318781.

References

- [1] Yin, P., Esser, E., Xin, J.: Ratio and difference of ℓ_1 and ℓ_2 norms and sparse representation with coherent dictionaries. *Communications in Information and Systems* **14**(2), 87–109 (2014)
- [2] Rahimi, Y., Wang, C., Dong, H., Lou, Y.: A scale-invariant approach for sparse signal recovery. *SIAM Journal on Scientific Computing* **41**(6), 3649–3672 (2019) <https://doi.org/10.1137/18M123147X>
- [3] Attouch, H., Bolte, J., Svaiter, B.F.: Convergence of descent methods for semi-algebraic and tame problems: proximal algorithms, forward–backward splitting, and regularized gauss–seidel methods. *Mathematical Programming, Series A* **137**(1–2), 91–129 (2013) <https://doi.org/10.1007/s10107-011-0484-9>
- [4] Beck, A., Teboulle, M.: A fast iterative shrinkage-thresholding algorithm for linear inverse problems. *SIAM Journal on Imaging Sciences* **2**, 183–202 (2009)
- [5] Bolte, J., Sabach, S., Teboulle, M.: Proximal alternating linearized minimization for nonconvex and nonsmooth problems. *Mathematical Programming* **146**(1–2), 459–494 (2014) <https://doi.org/10.1007/s10107-013-0701-9>

- [6] Chambolle, A., Pock, T.: A first-order primal-dual algorithm for convex problems with applications to imaging. *Journal of Mathematical Imaging and Vision* **40**, 120–145 (2011)
- [7] Combettes, P., Wajs, V.: Signal recovery by proximal forward-backward splitting. *Multiscale Modeling and Simulation: A SIAM Interdisciplinary Journal* **4**, 1168–1200 (2005)
- [8] Li, Q., Shen, L., Xu, Y., Zhang, N.: Multi-step fixed-point proximity algorithms for solving a class of optimization problems arising from image processing. *Advances in Computational Mathematics* **41**(2), 387–422 (2015)
- [9] Micchelli, C.A., Shen, L., Xu, Y.: Proximity algorithms for image models: Denoising. *Inverse Problems* **27**, 045009–30 (2011)
- [10] Parikh, N., Boyd, S.: Proximal algorithms. *Foundations and Trends in Optimization* **1**, 123–231 (2014)
- [11] Beck, A., Teboulle, M.: A fast iterative shrinkage-thresholding algorithm for linear inverse problems. *SIAM Journal on Imaging Sciences* **2**(1), 183–202 (2009) <https://doi.org/10.1137/080716542>
- [12] Tao, M.: Minimization of $\| \cdot \|_1$ Over $\| \cdot \|_2$ for Sparse Signal Recovery with Convergence Guarantee. *SIAM Journal on Scientific Computing* **44**(2), 770–797 (2022) <https://doi.org/10.1137/20M136801X>
- [13] Jia, J., Prater-Bennette, A., Shen, L.: Computing Proximity Operators of Scale and Signed Permutation Invariant Functions. *Journal on Optimization Theory and Applications* (arXiv:2404.00713) (2025, accepted) <https://doi.org/10.48550/arXiv.2404.00713> [math]
- [14] Martínez, J.M.: Local Minimizers of Quadratic Functions on Euclidean Balls and Spheres. *SIAM Journal on Optimization* **4**(1), 159–176 (1994) <https://doi.org/10.1137/0804009>
- [15] Tao, P.D., An, L.T.H.: Lagrangian stability and global optimality in nonconvex quadratic minimization over Euclidean balls and spheres. *Journal of Convex Analysis* **2**(1-2), 263–276 (1995)
- [16] Sherman, J., Morrison, W.J.: Adjustment of an Inverse Matrix Corresponding to a Change in One Element of a Given Matrix. *The Annals of Mathematical Statistics* **21**(1), 124–127 (1950) <https://doi.org/10.1214/aoms/1177729893>
- [17] Chávez-Pichardo, M., Martínez-Cruz, M.A., Trejo-Martínez, A., Martínez-Carbajal, D., Arenas-Resendiz, T.: A Complete Review of the General Quartic Equation with Real Coefficients and Multiple Roots. *Mathematics* **10**(14), 2377 (2022) <https://doi.org/10.3390/math10142377>